SURFACE AND MAGNETIC POLARITIONS ON NANODISK-ALIGNED MULTILAYER STRUCTURE

by

Zhijian Zhang

B. S. in Physics, Nanjing University, 2006

M. S. in Physics, Nanjing University, 2009

Submitted to the Graduate Faculty of

Swanson School of Engineering in partial fulfillment

of the requirements for the degree of

Master of Science

University of Pittsburgh

2011

UNIVERSITY OF PITTSBURGH

SWANSON SCHOOL OF ENGINEERING

This thesis was presented

by

Zhijian Zhang

It was defended on

March 29th, 2011

and approved by

Bong Jae Lee, PhD, Assistant Professor

Albert To, PhD, Assistant Professor

Mark Kimber PhD, Assistant Professor

Thesis Advisor: Bong Jae Lee, PhD, Assistant Professor

SURFACE AND MAGNETIC POLARITIONS ON NANODISK-ALIGNED MULTILAYER STRUCTURE

Zhijian Zhang, M. S.

University of Pittsburgh, 2011

In this thesis, the nanodisk-aligned multilayer structure, in which square cross-sectional nanodisks are vertically aligned on the top of a two-dimensional, dielectric-layered metallic structure, is proposed to investigate the near-filed and far-field radiative property enhancement for metamaterials. Multiple kinds of plasmonic resonances which support the peculiar properties of metamaterials have been identified on this proposed structure. Every plasmonic mode is analyzed and studied respectively. The localized plasmonic modes (Localized Surface Plasmon and Magnetic Polariton) are shown to be independent of the incidence angle and polarization, while the propagating plasmonic mode (Surface Plasmon) is demonstrated to be shifted with the varying of the incidence angle, which provides the possibility to make the plasmonic modes interact or couple with each other. The coupled plasmonic modes which are named as hybridized plasmonic modes can also be excited and lead to even more spectacular radiative properties both in the near-field and far-field.

The results obtained from this study suggest a novel model to explore the underlying mechanism of plasmonic resonances, especially for their hybridization. The study will advance our fundamental understanding of light-matter interaction at nanometer scale and will provide us more degrees of freedom to manipulate the radiative properties in both the near-field and far-field which might have great potentials in renewable energy applications that require specific radiative properties, such as thermophotovoltaic, photovoltaic cells and thermal emission sources.

TABLE OF CONTENTS

LIST OF EQUATIONS

LIST OF FIGURES

ACKNOWLEDGEMENT

I am heartily thankful to my supervisor, Dr. Bong Jae Lee, whose encouragement, guidance and support enable me to finish this thesis and my M. S. study. His instructive edification has inspired me to improve myself in the future research. In addition, I want to thank my other dissertation committee members, Dr. Albert To and Dr. Mark Kimber for their support and willingness to serve as a committee member.

Meanwhile, I would like to show my great appreciation to Dr. Minking K. Chyu for his invaluable advices for my career and sharing his experience and insight.

I also need to thank my colleague, Lina Xu, for her help in research and in daily life.

Moreover, I owe my deepest gratitude to my parents for their continuous support and dedication.

Finally, I want to dedicate this thesis to my fiancée Chenlu Wang. Her unconditional love is always my greatest impetus.

1.0 INTRODUCTION

Recently people have drawn much attention to achieve designable radiative properties (e.g., reflectance, transmittance and absorptance) by metamaterials, which indicates man-made materials with properties that may not be found in nature. Beneath the interest is the great potential to engineer the nanostructure in many promising applications. For instance, superlens [1] and plasmonic nanolithography [2] are proposed for breaking the diffraction limit with the help of metamaterials. With regards to device size decreasing, optical antenna [3] and plasmon waveguides [4] have been investigated. Moreover metamaterials provide extra possibilities for energy conversion, such as solar cells [5] and thermal emitters [6,7]. Triggered by the prospective potentials mentioned above, people drill down to the mechanism of metamaterials and study the elements from which the exotic response functions of metamaterials originate.

In the area we focus, metamaterials especially indicate optical metamaterials. That means the kind of materials we can tune their optical properties arbitrarily. The most important parameter of optical properties is the refractve index n. The refractive index, or in the other words index of refraction, of a substance is a measure of the speed of light in that substance. It is expressed as a ratio of the speed of light in vacuum relative to that in the considered medium. From the material point of view, the refractive index comes from two parts: permittivity ϵ, the electric response of a substance to the incident light, and permeability μ, the magnetic response of a substance to the incident light. The relationship is given by:

$$n = \sqrt{\epsilon\mu} \tag{1.1}$$

In nature, both ϵ and μ are mostly positive, thus the refractive index n is usually positive as well. Nevertheless, the greatest potential of optical metamaterials is the possibility to create a structure with a negative refractive index, which requires an effective negative ϵ and an effective negative μ. Materials with the negative refractive index, which are called negative index materials (NIMs), own many attracting features. As depicted in Fig 1-1(a), if the refractive index of the second medium is negative, light incident from a conventional positive index material (PIM) to a NIM will be refracted to the same side as the incidence. Furthermore, if light can be bent negatively, then a planar slab of a NIM inserted into a PIM space can focus light as shown in Fig 1-1(b).

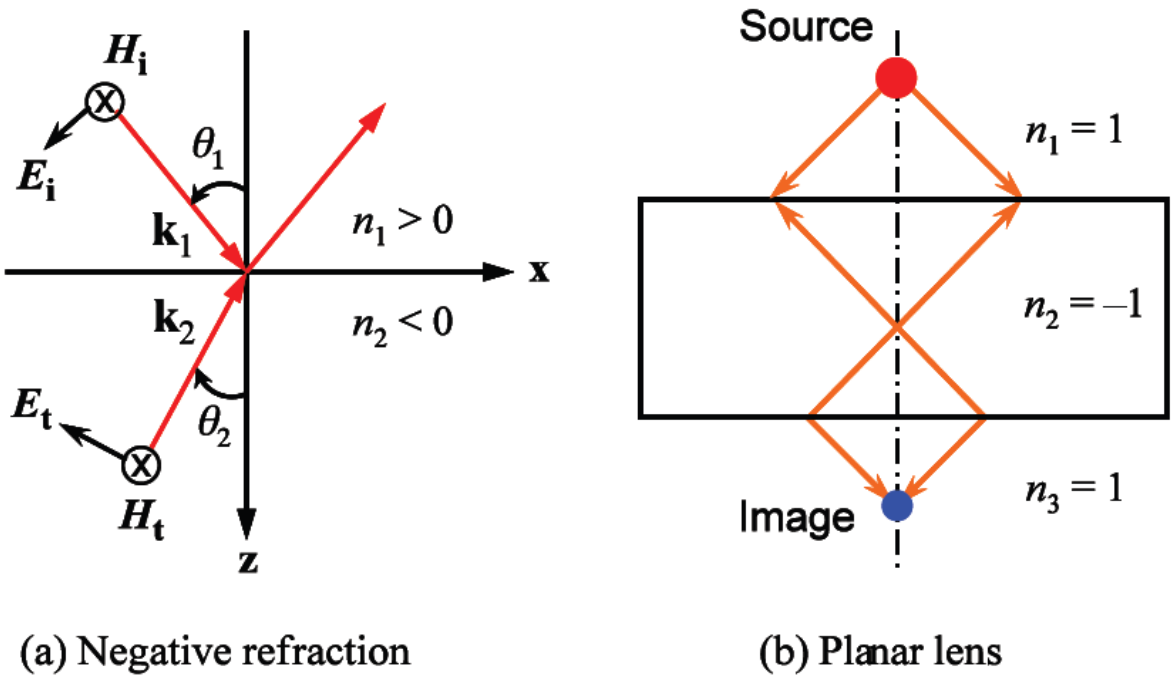

Fig 1-1, Unique features of a negative index material [8]: (a) negative refaraction and (b) planar lens

NIMs require electric and magnetic resonances separately in order to achieve abnormal permittivity and permeability different from unity. Electric resonance, which is relative to abnormal permittivity, includes surface plasmon polariton (SPP) or called surface plasmon (SP) [9] and localized surface plasmon (LSP) [10]. On the other hand, magnetic resonance corresponds to abnormal permeability which includes magnetic polariton (MP) [11].

A surface plasmon is a collective excitation of the electrons at the interface between dielectric and conductor. It can be excited by incident light on the periodically nano/micro-structured dielectric-conductor interface where the free space wave vector k_0 can be compensated by reciprocal lattice vector $\vec{G}_x = \frac{2\pi}{\Lambda_x}\vec{e}_x$, $\vec{G}_y = \frac{2\pi}{\Lambda_y}\vec{e}_y$. Moreover, the incident light can also induce the collective oscillation of free electrons in subwavelength objects, which is called localized surface plasmon. When the frequency of the incident light is resonant with the eigen frequency of the collective electron oscillation, the LSP is exited. On the other hand, magnetic polariton is the coupling of magnetic oscillation with incident light on material surface. It can be excited if the local structure supports the diamagnetism electron current on the surface of the material.

While Ebbesen *et al.* [12] demonstrated the extraordinary optical transmission through a two-dimensional array of subwavelength holes perforated on a silver film, the investigations on surface plasmon have been rekindled. SP has been studied in many different kinds of structures, like 1-D grating [13], 2-D hole array [14], bull's eye structure [15], and binary plasmonic structure [16]. In aforementioned periodic structures, the reciprocal wave vector should be applied to compensate the missing momentum between surface plasmon and incident light, which makes the transmission peaks resulting from SP are sensitive to the incidence angle and the precocity of the structure.

For the solo hole on thin metal films, people also found the evidence of surface plasmon, called localized surface plasmon [10]. By changing the geometric shape of the nano-holes, people investigate LSP theoretically [17] and experimentally [18,19]. LSP can also be supported by other subwavelength objects, such as nanoparticles [20,21]. On the nanoparticles, the resonance of charge density couples with incidence light, which leads to the existence of LSP. Those researches have shown that LSP is mostly dependent on geometrical shape of the resonators instead of periodicity or incidence angle.

Magnetic polariton has been studied even more, because it can support the artificial permeability. In order to get the negative permeability, J. B. Pendry [22] first proposed to use a split-ring resonator (SRR), to achieve diamagnetism. After that, magnetic resonance is widely studied. People successfully employ the single split-ring [23] and U-shape cells [24] to be the magnetic resonators. By using the anti-parallel currents in different metal layers, people fulfill magnetic resonance with paired metal strips [25]. Shalaev *et al.* explained the paired metal strips with the concept of MP [26], and later they also draw out the contribution of electric resonances [27,28]. Further, double-layered and multilayered fishnet structure [29,30] are discovered to be a very good candidate for bulk negative refraction index materials (NIM). Recently metal gratings and an opaque metallic film spaced by a dielectric spacer is suggested by Lee *et al.* [31]. This finding can be applied on enhancing the performance of a thermal emitter or thermal collector. Theoretically, people use inductor-capacitor circuit (LC) model to predict the fundamental resonance frequency of MP [29]. And, Lee *et al.* also analyzed the higher order MP situation.

SP, LSP, MP, those plasmonic resonances give different contributions for the metamaterials, yet they can also couple with themselves and interact with other kinds of resonances, which will dramatically change the optical properties of metamaterials. The hybridization of different kinds

of LSP has been investigated [32]. The interaction between LSP and SP is also considered [33]. It is well known that radiation loss of a magnetic dipole is substantially lower than that of an electric dipole of similar size [34], thus the coupling of MPs are even more widely studied. The early investigation involves coaxial SRRs [35]. After that, stereo-SRR dimer metamaterials are as well present [36]. MPs hybridization is also investigated on stacked cut-wire metamaterials [37] and tri-rod structure [38]. Moreover, the substructures in double layered fishnet materials are treated as magnetic atoms to study the coupling of MPs [39].

Based on what we have previously discussed, plasmonic resonances, SP, LSP and MP, are the keys to study metamaterials. However, in most of the former studies, plasmonic resonances are investigated separately, and their couplings need to be studied more. While related to the previous works mentioned above, this paper proposes a novel two dimensional (2D) nanodisk-aligned multilayer system, on which SP, LSP and MP can be studied and tuned at the same time. Moreover, the SP, LSP and MP on this structure can interact with each other and present coupled modes. Therefore, the study of our proposed structure will advance our understanding of the underlying mechanism of metamaterials and the light-matter interaction at nanometer scale.

On the other hand, radiative properties of micro/nanostructures for renewable energy applications should be designed for a broad spectral range as well as angle independence, and polarization independence. That is because thermal radiation from a hot object is unpolarized and randomly directed. A simple one-dimensional grating can only satisfy the requirements for a specific direction and polarization state. Yet, in real world applications, a two-dimensional structure will be desirable for the best performance under the irradiation from a hot object. Different from the former studies to enhance radiative properties which have mainly focused on one dimensional (1D) nanostructure for simplicity in modeling and manufacturing, the localized

plasmonic modes (MP and LSP) generated in our proposed structure can present radiative property enhancement which is indeed independent of incidence angle and polarization. Furthermore, the hybridization of the plasmonic resonances implies that we can manipulate the radioactive properties as well as near-field electromagnetic field distributions with more degrees of freedom. All these features of the proposed structure mean the potentials for renewable energy applications which require for a broad spectral range and angle independence, such as thermophotovoltaic, photovoltaic cells and thermal emission sources.

The thesis is structured as follows: in Chapter 2, we introduce the investigation theory we applied to the system, called rigorous coupled-wave analysis (RCWA). We expand it to 2D cases and verified it with 1D situation. In Chapter 3, the nanodisk-aligned multilayer structure as the system used to analyze the hybridization of MP, LSP and SP is described. The basic results from 2D RCWA is presented. In Chapter 4, the role of MPs on nanodisk-aligned multilayer system is discussed in detail. In Chapter 5, LSP and SP are investigated on our structure and asymmetric structure is introduced to verify the contribution of LSP and SP. Finally, some conclusions are given in Chapter 6.

2.0 THEORETICAL METHOD

In this chapter, the theoretical method we apply to this thesis, rigorous coupled-wave analysis (RCWA) is introduced. We extend the RCWA method from one dimensional (1D) to two dimensional (2D). The 2D method is verified by reproducing and comparing with 1D case.

Two-Dimensional Rigorous Coupled-wave Analysis

Rigorous wave-coupled analysis (RCWA) is a numerical modeling algorithm to solve Maxwell's equations for the electromagnetic wave diffracted in periodic structures. RCWA algorithm is wildly used in plasmonic optics study because of its good convergence and accuracy, especially when the grating's period is of the same order of magnitude as the wavelength. The accuracy of the solution provided by RCWA solely depends on the order of the space-harmonic expansion of the field. Therefore it is easy to balance the computation time and accuracy.

RCWA for the 1D structure is well developed [40,41], however in 2D case RCWA is still under investigation [42]. In this thesis, we extend 1D RCWA code to 2D situation and apply it into nanodisk-aligned multilayer structure.

To illustrate 2D RCWA, consider the periodic structure shown a unit cell as in Fig 2-1. The space is divided into 3 regions: Ⅰ incident region, Ⅱ grating region and Ⅲ transmitted region. The grating region can be structured by different layers, yet in each layer the permittivity is independent of *z*. By eliminating the *z*-dependency of the permittivity, it is possible to write

the solution inside each layer as a Fourier expansion, since only a dependency on the periodic coordinate *x*-*y* is present. At the boundaries between two layers, the tangential components of the electromagnetic fields are continuous. In this way, the unknown reflection and transmission coefficients of the incident region and transmitted region can be connected to each other and determined. For simplicity, we treat the situation for grating region as only one layer to illustrate 2D RCWA, though it can be composed of layers by layers as Fig 2-1 shows.

For 2D grating with periods of Λ_x andΛ_y, let's consider $\pm D_x$ and$\pm D_y$ diffraction orders to x and y direction, respectively. Based on the Floquet condition, we have diffraction wave vectors in *x*-direction and *y*-direction as

$$k_{xm} = k_x + \frac{2\pi}{\Lambda_x} m \ (-D_x < m < D_x)$$

$$k_{yn} = k_y + \frac{2\pi}{\Lambda_y} n \ (-D_y < n < D_y) \tag{2.1}$$

Where m and n are the diffraction orders, andk_x, k_y are the *x*-component and *y*-component of the incident wave vector.

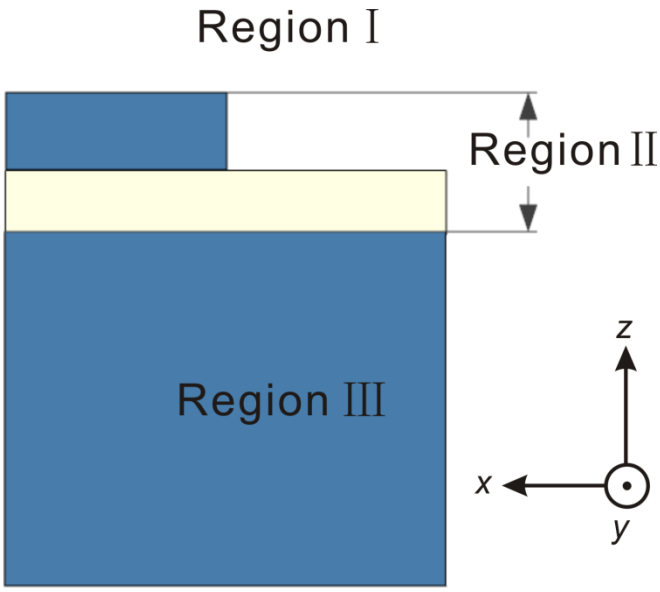

Fig 2-1. The sketch for the region division in RWCA

Hence, the normal wave vector component corresponding to each diffraction orders in Region Ⅰ and Region Ⅲ can be found from

$$k_{1zmn} = \sqrt{k_0^2\epsilon_1 - k_{xm}^2 - k_{yn}^2}$$

$$k_{3zmn} = \sqrt{k_0^2\epsilon_3 - k_{xm}^2 - k_{yn}^2} \tag{2.2}$$

where ϵ_1 and ϵ_3 is a dielectric function in Region Ⅰ and Region Ⅲ, respectively. Due to the periodicity, the dielectric function in the grating region can be expressed as Fourier series:

$$\epsilon(x,y) = \sum_m \sum_n \epsilon_{mn} exp\{i(\frac{2m\pi}{\Lambda_x}x + \frac{2n\pi}{\Lambda_y}y)\} \tag{2.3}$$

where ϵ_{mn} can be determined by the inverse Fourier transform.

The electric field in Region Ⅰ and Region Ⅲ can be expressed by a superposition of diffracted waves:

$$\vec{E}_1 = \vec{E}_i\, exp\{i(k_x x + k_y y + k_z z)\} + \sum_m \sum_n \vec{R}_{mn} exp\{i(k_{xm}x + k_{yn}y + k_{1zmn}z)\}$$

$$\vec{E}_3 = \sum_m \sum_n \vec{T}_{mn} \exp\{i(k_{xm}x + k_{yn}y + k_{1zmn}z)\} \tag{2.4}$$

Also, the electric and magnetic field in the grating region (i.e., Region Ⅱ) can be expressed as a Fourier expansion in terms of the spatial harmonics:

$$\vec{E}_2 = \sum_m \sum_n \vec{S}_{mn} exp\{i(k_{xm}x + k_{yn}y)\}$$

$$\vec{H}_2 = \frac{ik_0}{\omega\mu_0} \sum_m \sum_n \vec{U}_{mn}\, exp\{i(k_{xm}x + k_{yn}y)\} \tag{2.5}$$

where $k_0 = \frac{2\pi}{\lambda}$ with λ being the wavelength in vacuum. Note that $\vec{S}_{mn}$ and $\vec{U}_{mn}$ are related via Maxwell's equation. Consequently, one can derive the coupled differential equation for $\vec{S}_{mn}$ and $\vec{U}_{mn}$. Then the problem become as the eigen value problem for $\vec{S}_{mn}$ and $\vec{U}_{mn}$ with the boundary

condition that the tangential components of the electromagnetic fields at each region are continuous. Once $\vec{S}_{mn}$ and $\vec{U}_{mn}$ are solved, the unknown reflection and transmission coefficients of the incident region and transmitted region can be obtained easily.

For the ideal RCWA calculation, the diffraction orders m and n should be $\pm\infty$. Yet in the real application, the diffraction orders are truncated to be a finite number which can guarantee the convergence of the calculation.

The difficulty for 2D RCWA calculation is that it increases the computation time geometrically compare to the 1D situation. For instance, to calculate 1D grating with ± 10 diffraction orders, we need to solve eigenvalue and eigenvector of a complex matrix whose dimension is (2×21) by (2×21). However, to calculate 2D grating with ± 10 diffraction orders, we need to solve eigenvalue and eigenvector of a complex matrix whose dimension is (2×21^2) by (2×21^2). Thus the computation time is hugely increased. To balance the computation time and the accuracy, we choose the order of ± 18 in our 2D RCWA calculation, while the order of ± 19 has been chosen in a former work and shows reasonable convergence [42]. In their study, the absolute error is within 0.01 and the relative error is less than 5% when the diffraction order changes from ± 19 to the higher order of ± 25.

The extended 2D RCWA is applied to calculate the reflectance of 1D periodic strip-aligned multilayer structure as Fig 2-2 shows, where silver grating are aligned on a silicon dioxide film based on a silver substrate. The structure is under normal incidence and the electric field of the incident light is along *x*-direction. For comparison, 1D RCWA is also employed. The two results are shown in Fig 2-3. As it shown, the two methods match very well, which verify the validation of our 2D RCWA code.

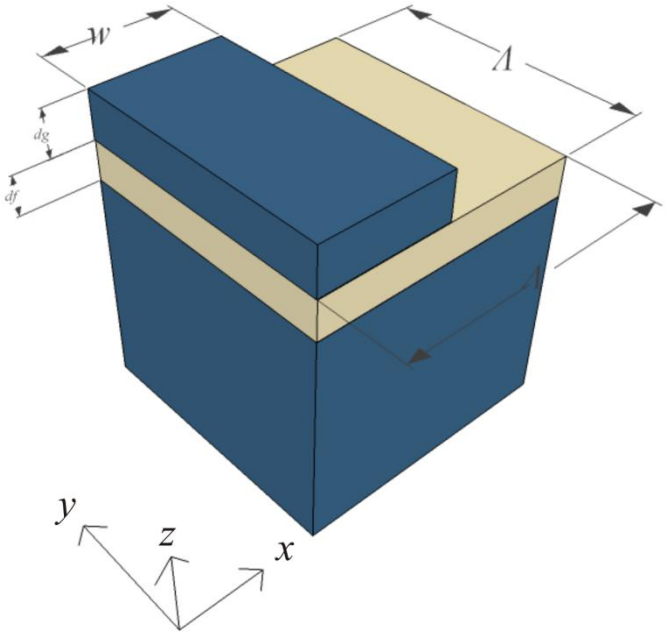

Fig 2-2, sketch for one unit cell of the 1D periodic strip-aligned multilayer structure. Λ*=500 nm,* d_f*=20 nm,* d_g*=20 nm, w=250 nm.*

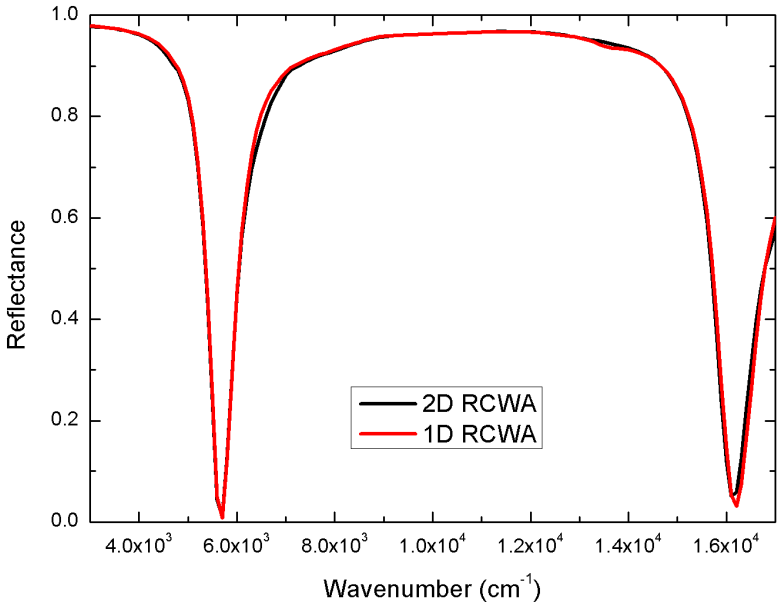

Fig 2-3, the reflectance of the structure in Fig 2-2, calculated by 2D RCWA code, compared with 1D RCWA code.

3.0 NANODISK-ALIGNED MULTILAYER STRUCTURE

In this chapter, the 2D nanodisk-aligned multilayer structure is presented, on which we apply 2D RCWA to study its radiative property. The reflectance spectrum result for normal incidence is shown and the meaning of each characteristic dip is provided.

2D Nanodisk-Aligned Multilayer and Reflectance Spectrum

One unit cell of the proposed 2D nanodisk-aligned multilayer structure is depicted as Fig 3-1. The square cross-sectional nanodisks are vertically aligned on the top of two-dimensional, dielectric-layered metallic structure. The silver substrate can be regarded as opaque since its thickness is much larger than the radiation penetration depth. The following parameters are picked for the better performance of the plasmonic modes and their hybridization. The periodicity Λ for the nanodisks aligning is 500 *nm* for both *x*-direction and *y*-direction on the plate. The nanodisk is square with width *w=250 nm* and its thickness d_g is 30 *nm*. The thickness of the SiO_2 d_f is 25 *nm*. A linearly polarized electromagnetic wave is incident from air at the incidence angle θ. θ is rotated in *x*-*z* plane. And we define *p*-polarization as electric field paralleled with *x*-direction as Fig 3-1 shows and *s*-polarization as magnetic field paralleled with *x*-direction.

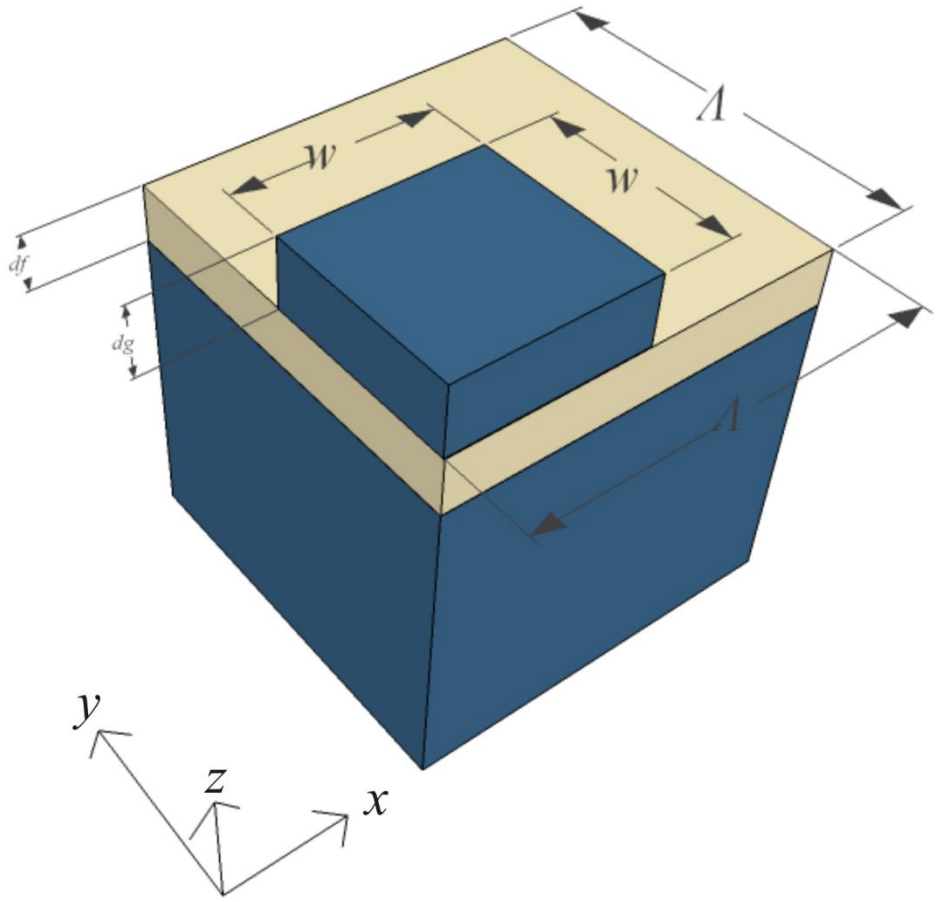

Fig 3-1, schematic of one unit cell for the proposed nanodisk-aligned multilayer structure. Λ *=500 nm,* d_f*=25 nm,* d_g*=30 nm, w=250 nm.*

We calculate the reflectance for the normal incidence in the wave number ranging from 5000 to 20000 cm^{-1} with 2D RCWA method. For normal incidence, the *s*-polarization and *p*-polarization are indistinguishable for this symmetric structure. The result is shown in Fig 3-2(a).

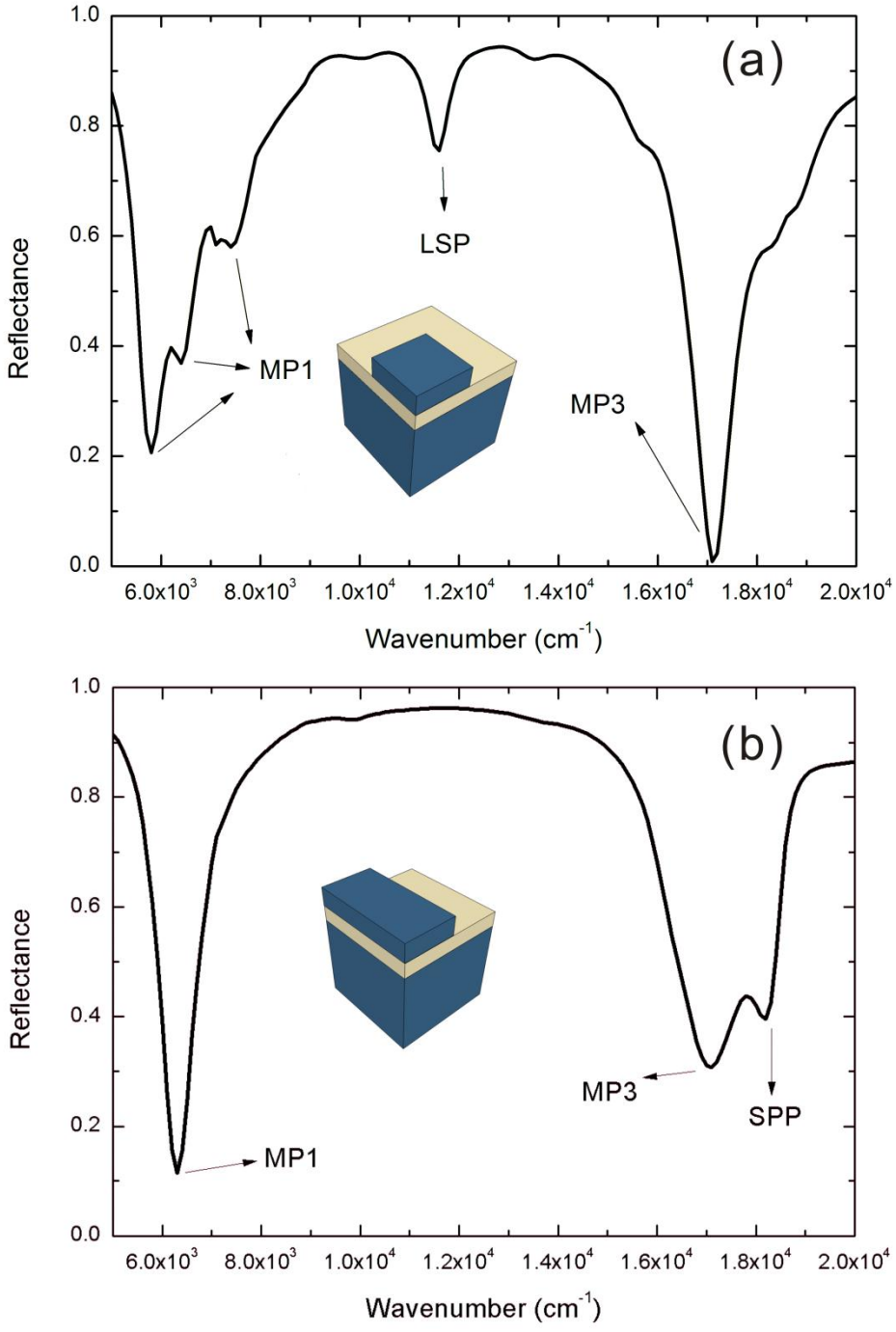

Fig 3-2, (a) reflectance of the proposed nanodisk-aligned multilayer structure for the normal incidence with *p*-polarization. (b) reflectance of the 1D periodic strip-aligned multilayer structure for the normal incidence with *p*-polarization.

The fundamental mode of MP (MP1) splits into 3 modes at 5800, 6400 and 7400 cm^{-1} in this nanodisk-aligned multilayer structure compared with the reflectance of 1D periodic strip-aligned multilayer structure (Fig 3-2(b)). The schematic of 1D periodic strip-aligned multilayer structure is the same as Fig 2-2 with different parameters of Λ *=500 nm,* d_f*=25 nm,* d_g*=30 nm, w=250 nm*. The 2D nanodisk-aligned multilayer structure supports localized surface plasmon (LSP) at 11600 cm^{-1} where the nanodisk stands as a nanoparticle and supports LSP by it alone. And this character cannot be found in 1D periodic strip-aligned multilayer structure. For the dip around 17200 cm^{-1} we will prove in the later chapter that it is the third order harmonic mode of MP (MP3), yet this MP3 mode is coupled with SP mode. For the reflectance of 1D periodic strip-aligned multilayer (Fig 3-2(b)), MP3 can be separated with SP, but they still interact with each other. And MP3 is shifted a little bit according to this coupling.

4.0 MAGNETIC POLARITON MODES

This Chapter provides the background knowledge of magnetic polariton (MP), which results in some basic characteristics for MPs. The properties of MPs on nanodisk-aligned multilayer are investigated according to the reflectance spectrums at different incidence angles and different polarizations. The field distribution for each characteristic mode is also presented to demonstrate the underlying physical mechanisms.

4.1 MAGNETIC POLARITON: BACKGROUND

Magnetic polariton by definition is the magnetic oscillation on material surface coupled with incident light, which depends mostly on the plasmonic properties and geometry structure of the material. It draws much attention because of its potential to achieve effective negative refractive index materials.

The key parameter for light interaction with matter is the refractive index ($n = n' + in''$). In nature, the real part of refractive index n' is always positive. However, many efforts are put to realize negative n' because of its great potentials for many amazing applications, such as superlen [1] and nanofabrication beyond diffraction limit [2]. The negative refractive index requires for negative permittivity and permeability. Those two parameters show how the matter

reacts with the incident electromagnetic wave. For permittivity, it is determined by the ability of a material to polarize in response to the field, in general the response reduces the total electric field inside the material. However, there can be abnormal response if electric resonance exists in the material, such as SP, LSP and plasma phenomenon for noble metals in the infrared and visible spectrums, which actually increase the total electric field. In this case, the real part of permittivity can be negative. For permeability, the situation is similar. Permeability is the amplitude of magnetization that a material obtains in response to the incident electromagnetic wave. In nature the response always decreases the total magnetic field in the material. Yet, in the case of existence of some abnormal magnetic resonance such as MP, the material response in fact enhances the total magnetic field, or it can be understood as strong diamagnetism occurs. Then the real part of permeability can be negative. Or in the other words, MP can support the existence of negative permeability. Once the MP exists, the total field is enhanced inside the material, which leads to energy localization according to the resonance. In that case, the absorptance α is largely enhanced. For our nanodisk-aligned multilayer structure, since the silver film is opaque (transmittance$T = 0$), from the energy conservation $R = 1 - \alpha$, one can observe reflectance dips by the attribution of the excitation of MPs. Thus in this thesis we can study the reflectance dips in the spectrums to investigate MPs.

According to Lenz's Law, when a time-varying magnetic field is parallel to axis of a spiral coil of metal wire, an induced magnetic field will occur due to resultant current in the coil. Therefore, diamagnetism is achieved. Based on this perspective, LC circuit model is often used to study the diamagnetism. The frequencies of the LC resonances are determined entirely by the geometry and size. In order to scale the diamagnetic response to the optical frequencies, where

the plasmonic properties are dominant, people also modify the effective geometry parameters and apply the LC circuit model to successfully describe and predict MP resonance [29].

In former studies, diamagnetism has been achieved by the single split-ring [23], U-shape cells [24], paired metal strips [25] and double-layered or multilayered fishnet structure [29, 30]. Recently 1D periodic strip-aligned multilayer structure is suggested by Lee *et al.* [31] to apply MP properties to enhance the performance of thermal emitter, thermal collector or photovoltaic cell.

Regarding the specific requirement of radiative properties, the design of renewable energy applications should be feasible to a broad spectral range as well as a wide angular region and it should be polarization independent. That is because thermal radiation from a hot object, such as the sun for a good illustration, is unpolarized and randomly directed. A simple one-dimensional grating can satisfy the requirements for a specific direction and polarization state. In real world applications, a two-dimensional (2D) structure will be desirable for the best performance under the irradiation from a hot object. Therefore, we introduce 2D nanodisk-aligned multilayer structure, on which the angle and polarization independent radiative properties can be supported by MP resonance.

4.2 MAGNETIC POLARITON ON NANODISK-ALIGNED MULTILAYER

The diamagnetism of the nanodisk-aligned multilayer structure can be explained as follows. The incident light produces oscillating magnetic field and this field induces a current in the nanodisk along the x direction and another near the surface of the metal film in the opposite direction. The

anti-parallel currents result in a diamagnetic response. The diamagnetic response is then coupled to the metallic film to cause the MP on the surface.

We calculate the reflectance for the nanodisk-aligned multilayer structure as illustrated in Chapter 3, which is under *p*-polarization incidence with different incidence angles, as shown in Fig 4-1. The periodicity Λ for the nanodisks aligning is 500 *nm* for both *x*-direction and *y*-direction on the plate. The nanodisk is square with width *w=250 nm* and its thickness d_g is 30 *nm*. The thickness of the SiO_2 d_f is 25 *nm*. As we can see, according to the extra confinement in the *y*-direction, the fundamental mode of MP on 2-D nanodisk-aligned multilayer structure splits into 3 modes at 5800, 6400 and 7400cm^{-1}, as shown in Fig 4-1. The *y*-direction magnetic field distributions on the surface of the silver substrate are calculated for those three dips and plotted in Figure 4-2. We can see that for all those three dips, the anti-parallel currents between the nanodisk and the substrate confine strong magnetic field inside the space covered by the nanodisk.

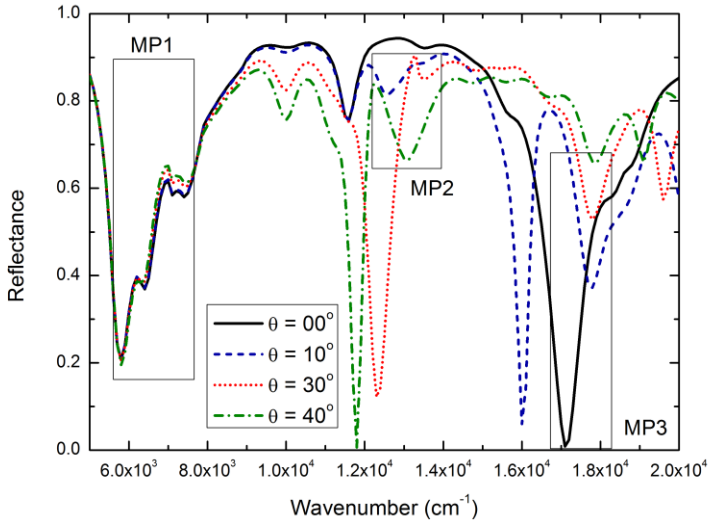

Fig 4-1, the reflectance of the proposed nanodisk-aligned multilayer structure for the different incidence angles. The incident lights are in *p*-polarization.

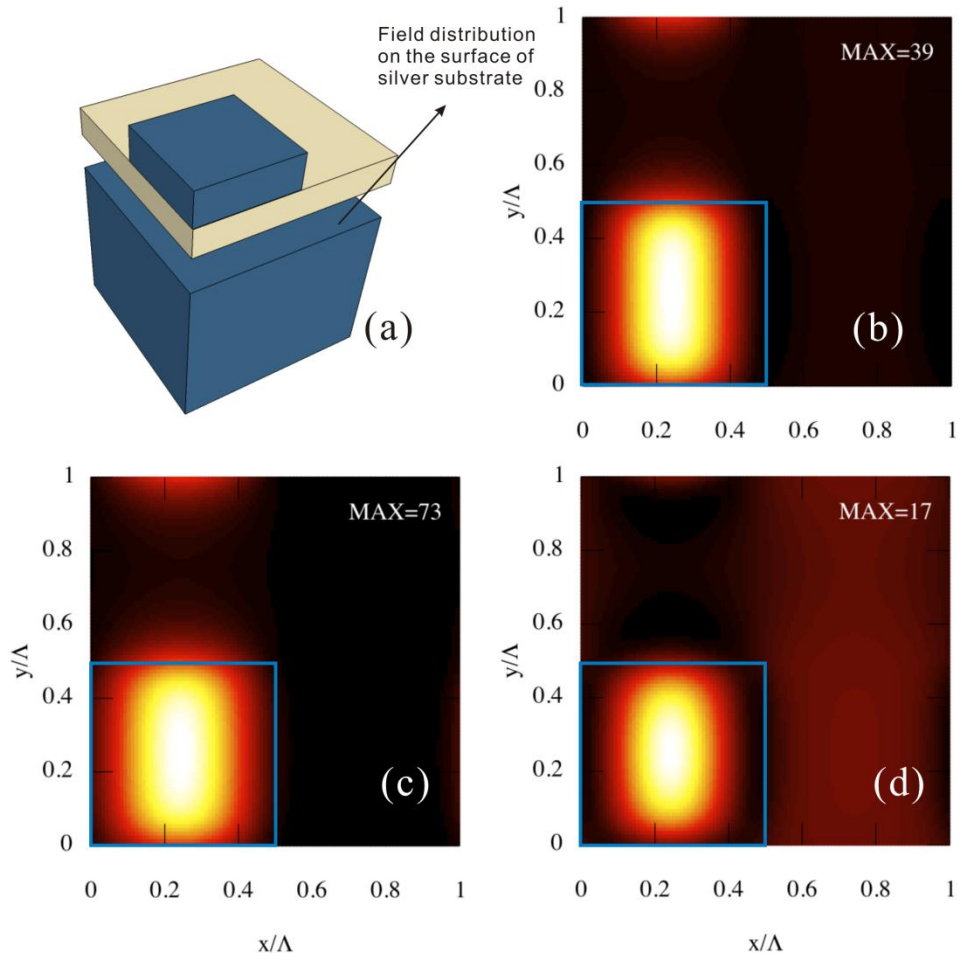

Fig 4-2, (a) schematic of the plane where the *y*-direction magnetic field distribution on the surface of the silver substrate is calculated; the field distribution for reflectance dips at 5800 (b), 6400(c) and 7400 cm^{-1} (d), while the incident light is normal to the surface. The magnetic field is normalized by the incidence magnetic field as $|H_y|^2/|H_{y,inc}|^2$. The brighter color implies the stronger field. "MAX" shows the maximum value of $|H_y|^2/|H_{y,inc}|^2$ in the plane. The blue square shows the position of the nanodisk.

And there is only one resonance loop for all those three modes, which demonstrates that all the dips are split MP1 modes. The deep physical reason for the splitting of the MP1 mode is still unclear, which need to be investigated in the future.

Besides the fundamental mode of MP, the third order harmonic mode (MP3) can also be excited for normal incidence at 17100cm^{-1}, as shown in Fig 4-1. We also calculate its magnetic field distribution in the *y*-direction on the surface of the silver substrate, as plotted in Fig 4-3. We can see that similar with MP1 modes, there is a strong magnetic field confined inside the space covered by the nanodisk. Yet, there are three resonance loops, which indicate that it is MP3 mode. We can also observe that the resonance is not so localized in the space covered by the nanodisk. We will demonstrate it results from the influence of surface plasmon (SP) in the later chapter.

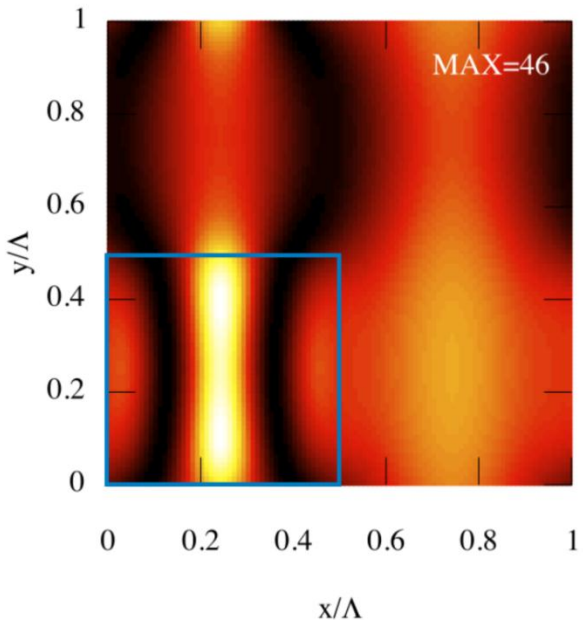

Fig 4-3, the y-direction magnetic field distribution on the surface of the silver substrate for reflectance dips at 17100cm^{-1}. The incident light is normal to the surface. The magnetic field is normalized by the incidence magnetic field as$|H_y|^2/|H_{y,inc}|^2$. The brighter color implies the stronger field. "MAX" shows the maximum value of $|H_y|^2/|H_{y,inc}|^2$ in the plane.

The second order harmonic mode (MP2) cannot be excited under the normal incidence. That is because the two anti-parallel current loops are strictly mirror symmetric for normal incidence, and the magnetic fields induced by the currents cancel each other out. In that case, MP2 mode cannot present [18]. However, for the oblique *p*-polarization incidences, the mirror symmetry of the two anti-parallel current loops is broken. Thus we could find MP2 mode dips in reflectance under oblique p-polarization incidence situation, as we can see in Fig 4-1. The dip at 12600 cm^{-1} for $\theta = 10^{\circ}$, the dip at 12300 cm^{-1} for $\theta = 30^{\circ}$ and the dip at 13100 cm^{-1} for $\theta = 40^{\circ}$ are all MP2 dips. We also show magnetic field distribution in the y-direction on the surface of the silver substrate in Fig 4-4 for the dip at 12600 cm^{-1} and incidence angle $\theta = 10^{\circ}$. These tow asymmetric resonance loop gives the evidence for MP2 mode.

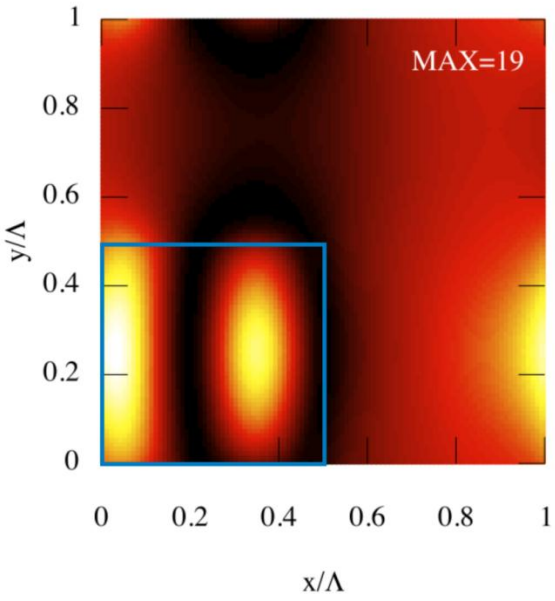

Fig 4-4, the y-direction magnetic field distribution on the surface of the silver substrate for reflectance dips at 12600 cm^{-1} under the incidence angle $\theta = 10^{\circ}$. The magnetic field is normalized by the incidence magnetic field as $|H_y|^2/|H_{y,inc}|^2$. The brighter color implies the stronger field. "MAX" shows the maximum value of $|H_y|^2/|H_{y,inc}|^2$ in the plane.

From the effective LC circuit model, we know the property of MPs depends only on the local geometry of the micro/nanostructure and the plasmonic property of the material which is intrinsic, thus we can say MPs are localized and the diffracted evanescent waves cannot affect them. In other words, if the materials are fixed, the resonance frequencies for MPs in our system depend only on the geometry of the nanodisk but remain unchanged with the unit cell period Λ and the incidence angle. To verify this, we calculate the oblique incidence situations for both *p*-polarization and *s*-polarization and compare them in Fig 4-5. For the normal incidence, *p*-polarization and *s*-polarization are indistinguishable, as shown in Fig 3-2. As the figures show, MP1 at 5800, 6400 and 7400cm^{-1}, for both *s* and *p* polarizations, MP2 around 12600~13100 cm^{-1} for *p* polarization, and MP3 around 17100~17900 cm^{-1} for both *s* and *p* polarizations, all these MP modes remain at almost unchanged frequencies while the incidence angle is changing. The slight changes for the dips under same MP modes are due to the interaction between MP and SP, which we will discuss later. As we noticed, the *s*-polarization cannot support MP2 modes. The schematic of the current for the assumptive MP2 mode under *s*-polarization incidence is shown in Fig 4-6. As we can see, because for *s*-polarization the incident electric field is parallel to the surface, the oblique incidence angle cannot break the mirror symmetric for the resonance loops and the total induced magnetic is effectively zero in this case.

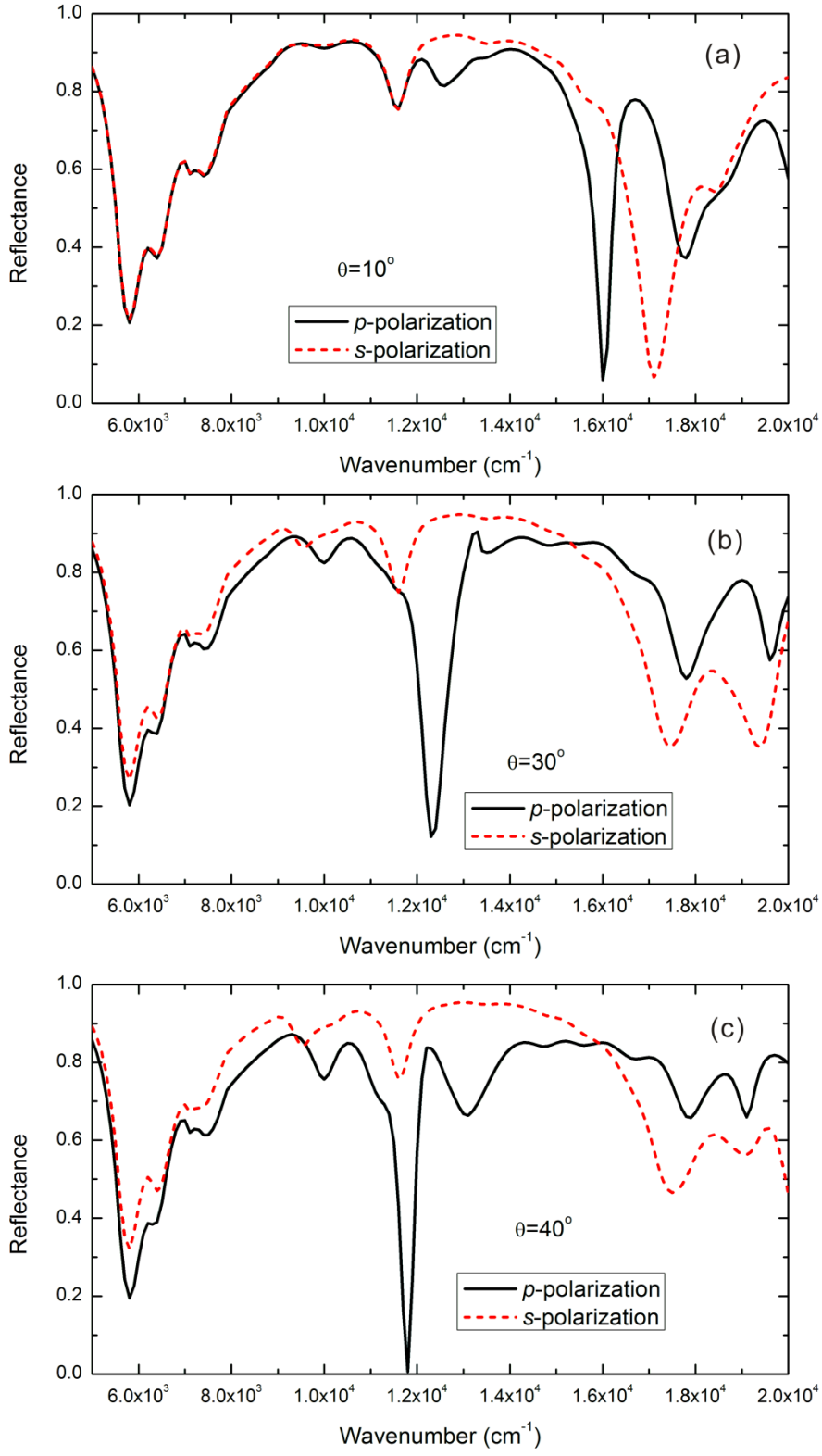

Fig 4-5, reflectance of the proposed nanodisk-aligned multilayer structure under different oblique incidence angles.

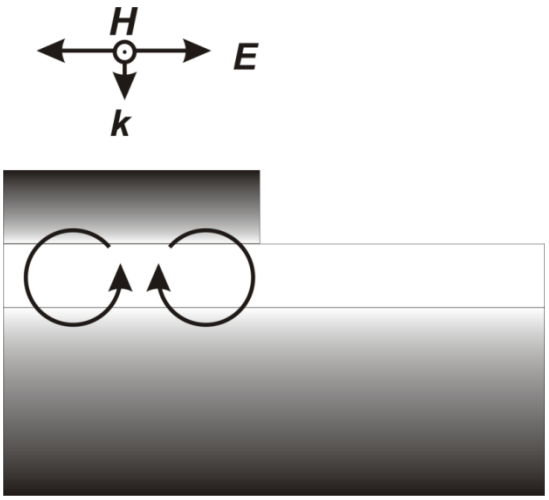

Fig 4-6, schematic of the current for the assumptive MP2 mode under *s*-polarization incidence

The primary advantage for the 2D proposed nanodisk-aligned multilayer structure, compared to 1D periodic strip-aligned multilayer structure, is that in the 2D structure, the MPs can be not only independent of the incidence angle but also independent of polarization of the incident light. We can easily check Fig 4-1 and Fig 4-5 to verify this. Thus, the true all-incident-angle radiative property enhancement can be achieved by nanodisk-aligned multilayer structure. Therefore, the proposed nanodisk-aligned multilayer structure is a big step closer to the real world applications for renewable energy, such as thermal emitter, thermal collector and photovoltaic cell.

5.0 SURFACE POLARITON MODES AND HYBRIDIZAITON

In this chapter, we discuss the characteristics about surface plasmon (SP), localized surface plasmon (LSP). The roles of SP and LSP played on nanodisk-aligned multilayer structure are studied by reflectance spectrum and the field distribution for each characteristic mode. We also investigate the coupling between SP and MP, SP and LSP on the system, and how these couplings affect the reflectance spectrum.

5.1 SURFACE PLASMON

A surface plasmon (SP) is a collective excitation of the electrons at the interface of dielectric and conductor. For the half-infinite dielectric and conductor interface, we could easily derive the dispersion of surface plasmon by applying Maxwell equation and boundary conditions [43].

$$k_{sp} = k_0 \sqrt{\frac{\varepsilon_d \varepsilon_m}{\varepsilon_d + \varepsilon_m}} \tag{5.1}$$

where k_0 is the free space wave vector, ε_d is the dielectric permittivity and ε_m is the metal permittivity .We could notice that the wave vector of SP k_{sp} is always larger than the free space wave vector ($k_{sp} > k_0$), which means that SP cannot be excited by the free space incident light on

the smooth dielectric-conductor surface. However, for nanodisk-aligned multilayer, the periodic structured dielectric-conductor surface supports high order diffraction. And then the reciprocal vector could supply the missing momentum which can excite SP.

$$\vec{k}_{sp} = \vec{k}_0 \sin\theta + (i\vec{G}_x + j\vec{G}_y) \tag{5.2}$$

where reciprocal lattice vector $\vec{G}_x = \frac{2\pi}{\Lambda_x}\vec{e}_x$, $\vec{G}_y = \frac{2\pi}{\Lambda_y}\vec{e}_y$.

We know SP is a kind of collective electron excitation. And it is companied with great field electromagnetic field enhancement on the surface of the material. This kind of energy confinement can also lead to dips in the reflectance spectrum. From Eq. 5.2, we know that the frequency of SP resonance depends on the incidence angle and the periodicity of the structure. And because no collective electron excitation can be coupled with the incident light for s-polarization, the s-polarization incident light cannot support SP resonance.

For the simplicity, we calculate the reflectance for simple grating, by setting d_f=0, in the case of 1D periodic strip-aligned multilayer structure shown in Fig 2-2. The incident light is in different angle. The characteristic SP modes on this simple grating structure represent for SP modes on 2D nanodisk-aligned multilayer, as long as they share the same periodicity and the incident light is p-polarization. The results are given is Fig 5-1. All the dips in the reflectance

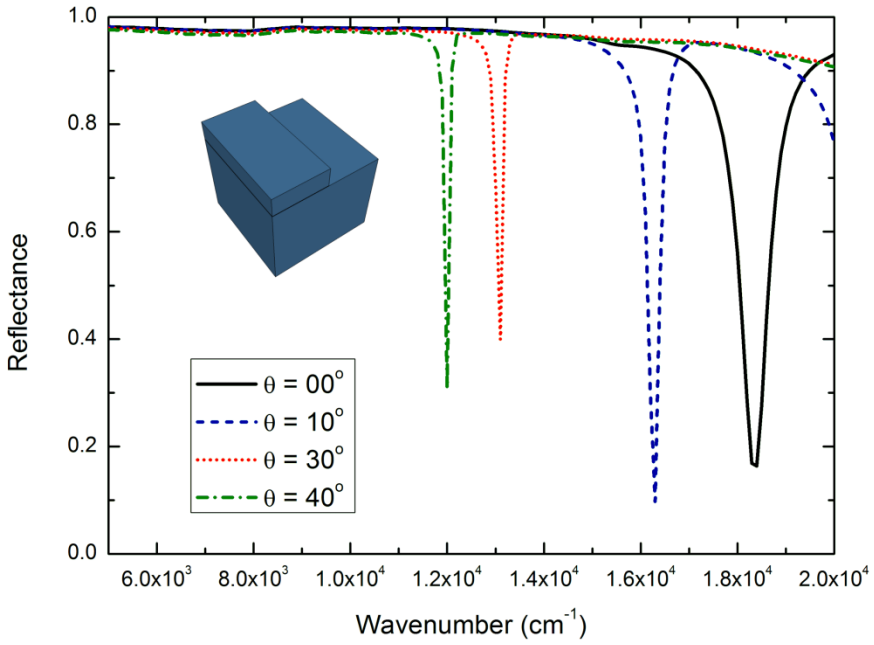

Fig 5-1, reflectance of 1D simple grating at different incidence angles. Λ*=500 nm,* d_f*=0 nm,* d_g*=30 nm*, *w=250 nm*. The incident lights are in *p*-polarization.

satisfy Eq. 5.2, and represent the (1,0) mode (*i*=1, *j*=0) SP for each different incidence angle. (1,0) mode and (0,1) mode are overlapped with each other. We can compare this calculation with 2-D nanodisk-aligned multilayer result and index out the 10 SP modes, as shown in Fig 5-2. We can see all the SP modes match with the simple grating calculation in a reasonable range, except for the normal incidence. For the normal incidence, there is no SP dip around the frequency which is predicted by equation (2) and by the simple grating calculation. The (1, 0) SP mode for the normal incidence is supposed to be around 18200 cm^{-1} , yet the MP3 mode is also around this frequency range that is close enough to couple with the SP mode. Thus these two modes couple with each other and support the dip at 17100cm^{-1}. We can find the MP3 mode for the normal incidence deviates from the other MP3 modes for the oblique incidences, yet all MP modes are

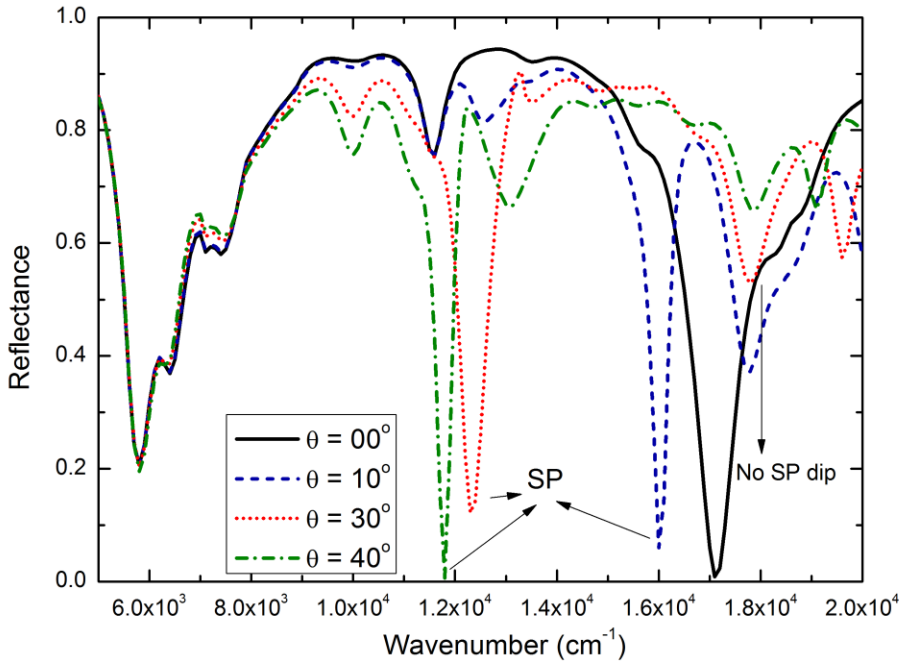

Fig 5-2， the reflectance of the propose 2D nanodisk-aligned multilayer structure for the different incidence angles. The incident lights are in *p*-polarization.

supposed to occur at a fixed frequency. The reason is also from the coupling of MP3 mode and SP mode. Only the SP mode for normal incident is close enough to MP3 mode to get them coupled. Besides, because the reflectance dip at 17800 cm^{-1} under normal incidence results from the coupling of SP mode and MP3 modes, the dip goes deeper than the uncoupled SP mode or pure MP3 mode.

To understand the physical mechanism of this coupled SP and MP3 mode, we calculate the *y*-direction magnetic field distribution on the surface of the silver substrate for pure SP mode (16000 cm^{-1} at $\theta = 10^{\circ}$ in Fig 5-3(a)), uncoupled MP3 mode (17800 cm^{-1} at $\theta = 10^{\circ}$ in Fig 5-3(b)), and coupled SP and MP3 mode ((17800 cm^{-1} at $\theta = 0^{\circ}$ in Fig 5-3(c)). As we can see, for

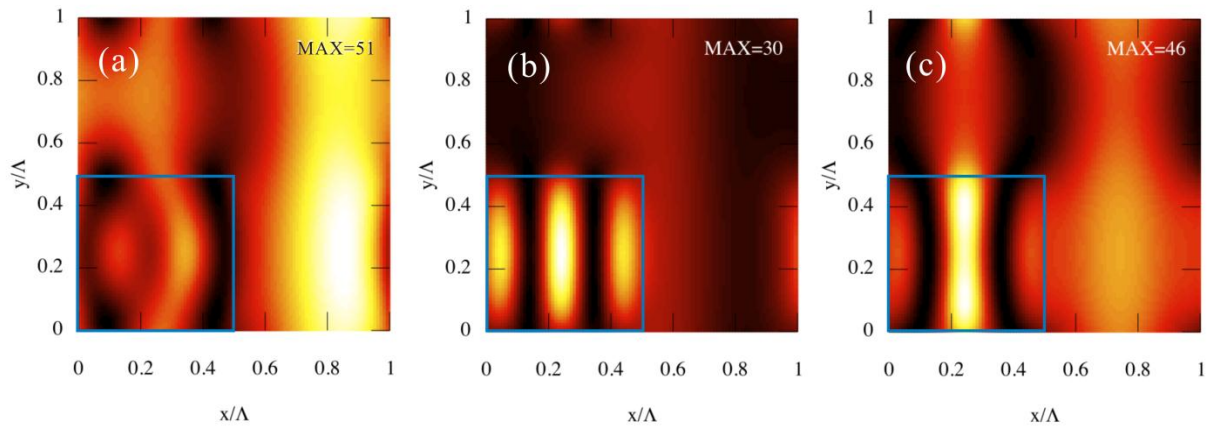

Fig 5-3, the *y*-direction magnetic field distribution on the surface of the silver substrate for reflectance dips at 16000 cm^{-1} while $\theta = 10^{\circ}$ (a); 17800 cm^{-1} while $\theta = 10^{\circ}$ (b); and 17100 cm^{-1} while $\theta = 0^{\circ}$ (c). The magnetic field is normalized by the incidence magnetic field as $|H_y|^2/|H_{y,inc}|^2$. The brighter color implies the stronger field. "MAX" shows the maximum value of $|H_y|^2/|H_{y,inc}|^2$ in the plane.

SP mode, the field is strong not only on the surface covered by the nanodisk but also almost everywhere on the surface. That is because SP modes are not localized on the plane. They are only localized in the z-direction, yet propagating on the surface. In contrast, the field for MP3 mode is mostly localized on the nanodisk covered surface and shown three resonance loops. The field distribution for coupled SP and MP3 mode shows combined characteristics of SP mode and MP3 mode. It owns both the localized three resonance loops under the surface covered by nanodisk and the enhanced field diffused everywhere on the surface. And we can understand the frequency shift of coupled SP and MP3 mode like this: the MP3 mode supports the localized three resonance loops under the surface covered by nanodisk However, when the SP mode occurs, the localized field is distracted by the field induced by SP in some degree. Thus, the resonance frequency decreases, and the wave number of resonance decreases correspondingly.

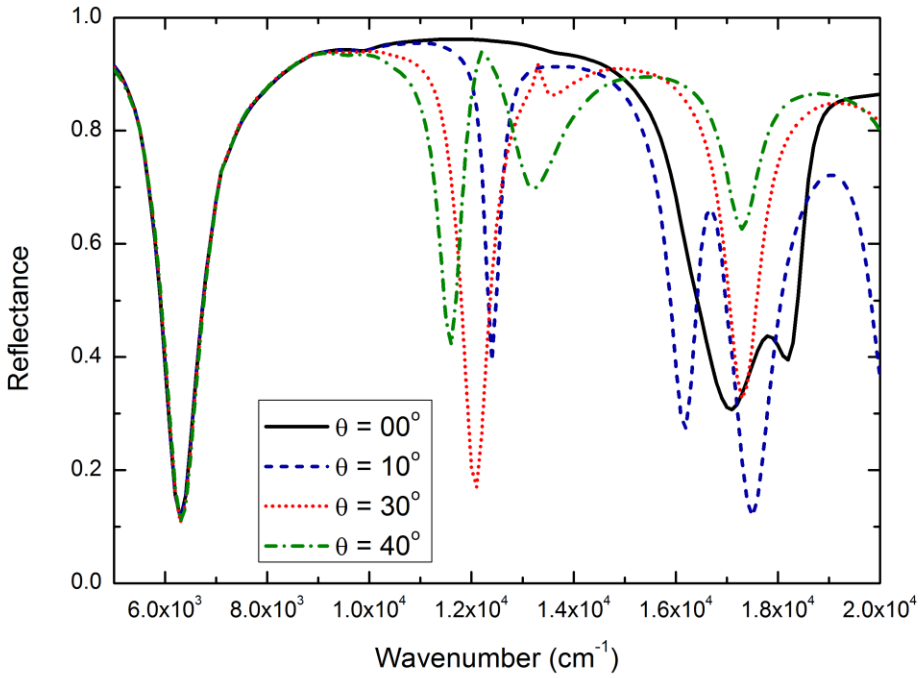

Fig 5-4， the reflectance of the 1D periodic strip-aligned multilayer structure at different incidence angles. The incident lights are in *p*-polarization.

To verify this coupling effect, we also calculate the reflectance for 1D periodic strip-aligned multilayer of the same parameters at different incidence angles as comparison in Fig 5-4. The SP mode for the normal incidence shows as a dip which is closed to the MP3 mode in this case, yet the MP3 mode for the normal incidence is affected by the SP mode so that it deviates from the other MP3 modes for the oblique incidences similar to the 2D case. Therefore, the similar coupling effects can present in both 1D periodic strip-aligned multilayer structure and 2D nanodisk-aligned multilayer structure.

So far, the coupling effects between MPs and SPs on nanodisk-aligned multilayer are demonstrated.

5.2 LOCALIZED SURFACE PLASMON

The incident light can induce the collective oscillation of free electrons in subwavelength objects such as metal nanoparticle, nanowire and nanodisk. While the frequency of the incident light is resonant with the eigen frequency of the collective electron oscillation, the localized surface plasmon (LSP) is exited. Like MPs, LSPs depend only on the local geometry of the nanoparticles and the intrinsic material property. Therefore it should as well be independent of the incidence angle and polarization. For the 2D nanodisk-aligned multilayer structure, the nanodisks can support LSP mode by themselves alone. We can find LSP modes on the reflectance of nanodisk-aligned multilayer both under p-polarization (Fig 5-2) and s-polarization (Fig 4-5) at 10000 cm^{-1} and 11600cm^{-1}, which are shown as independent of the incidence angle and polarization. We also calculate the field distribution for one LSP mode as an example. Because for LSP the field should be constrained around the nanodisk, we no longer choose the silver substrate surface to plot the field distribution. Instead, we choose the top surface of the nanodisk to plot the y-direction magnetic field distribution for the LSP mode at 11600 cm^{-1} in Fig 5-5. As the LSP characteristic predicts, the enhanced magnetic field is localized around the nanodisk.

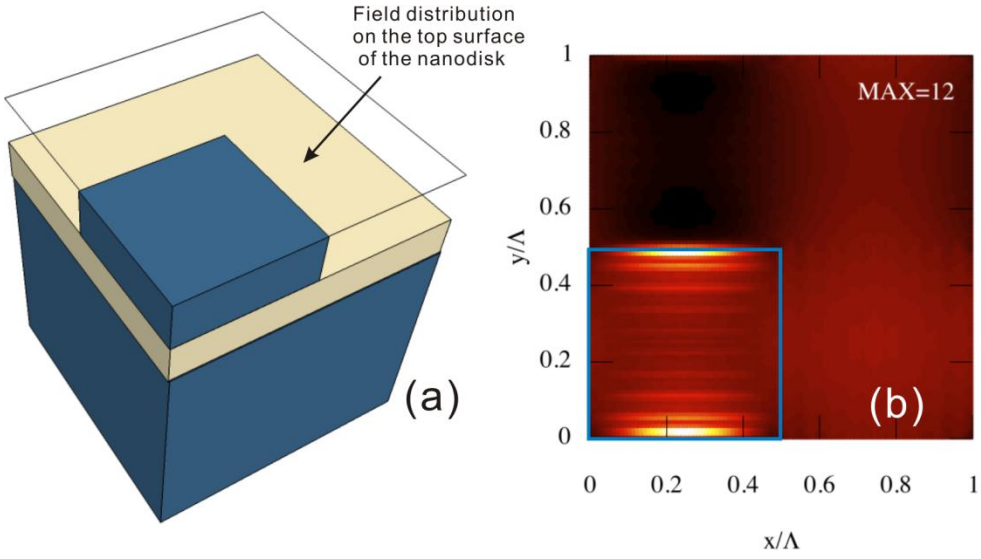

Fig 5-5, (a) schematic of the plane where the *y*-direction magnetic field distribution on the top surface of the nanodisk is calculated; (b) the field distribution on the top surface of the nanodisk for reflectance dips at 11600 cm^{-1} while $\theta = 0^{\circ}$. The magnetic field is normalized by the incidence magnetic field as $|H_y|^2/|H_{y,inc}|^2$. The brighter color implies the stronger field. "MAX" shows the maximum value of $|H_y|^2/|H_{y,inc}|^2$ in the plane.

To illustrate the dips at 10000 cm^{-1} and 11600 cm^{-1} result from LSP, we calculate the reflectance of nanodisk aligned on a free standing silicon dioxide film with all the same parameters of our nanodisk-aligned multilayer structure, except that there is no silver substrate. As we can see from Fig 5-6, the nanodisk-aligned silicon dioxide film also gives two dips at 10000 cm^{-1} and 11600 cm^{-1} in its reflectance. For this kind of structure, MP modes cannot be excited, because there is no structure which supports an effective diamagnetism current. And because the mode at 10000 cm^{-1} and 11600 cm^{-1} is angle and polarization independent, they should be among LSP modes and MP modes. After all, we can identify the dips at 10000 cm^{-1} and 11600 cm^{-1} are LSP resonance modes.

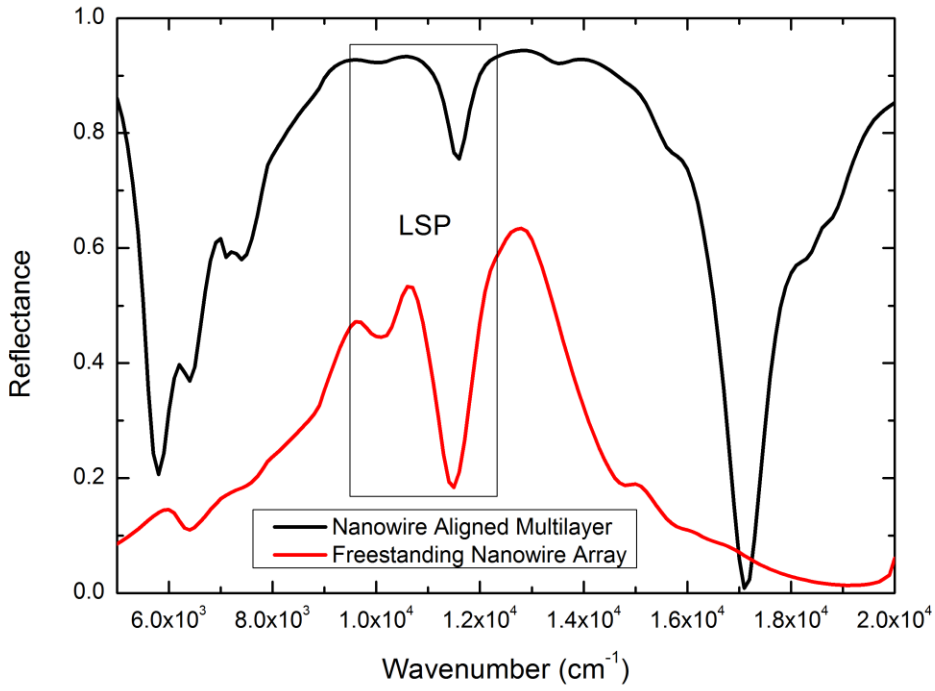

Fig 5-6, the reflectance of the nanodisk-aligned freestanding silicon dioxide film for the normal incidence (red) compared with the reflectance of nanodisk-aligned multilayer for the normal incidence (black).

Comparing the reflectance of 2D nanodisk-aligned multilayer Fig 5-2 with 1D periodic strip-aligned multilayer Fig 5-4, we find there is no LSP mode excited at 10000 cm^{-1} and 11600 cm^{-1} on periodic strip-aligned multilayer. That also verifies that those two modes come from the LSP excitation of nanodisks which cannot be supported on the strip structure.

LSP can also couple with SP and MP on the nanodisk-aligned multilayer. While under the incidence of p-polarization light, SP mode can be excited on the nanodisk-aligned multilayer. Because the frequency of SP mode varies with the incidence angle while the frequency of LSP

mode and MP mode are fixed, it is possible for SP mode to get close enough to LSP mode and MP mode in the reflectance spectrum to interact with each other by varying the incidence angle. From the Fig 5-2, the coupled LSP, MP and SP modes can be find at 12300 cm^{-1} under $\theta = 30^{\circ}$ and 11800 cm^{-1} under $\theta = 40^{\circ}$. For both these two situations, the SP modes which are supposed to happen at 13100cm^{-1} for $\theta = 30^{\circ}$ and 12000cm^{-1} for $\theta = 40^{\circ}$ are close enough to the LSP mode at 11600 cm^{-1} and MP2 mode around 12600cm^{-1}. Thus LSP, MP and SP modes are coupled with each other and present a dip which is stronger than the dip excited by LSP, MP or SP alone. For illustration, we calculate the *y*-direction magnetic field distribution on both the surface of silver substrate and the top surface of the nanodisk for the dip at 11800 cm^{-1} under $\theta = 40^{\circ}$ in Fig 5-7.

On the surface of silver substrate, the field distribution presents the characteristics of both MP2 and SP, which shows two asymmetric resonance loops localized in the area covered by the

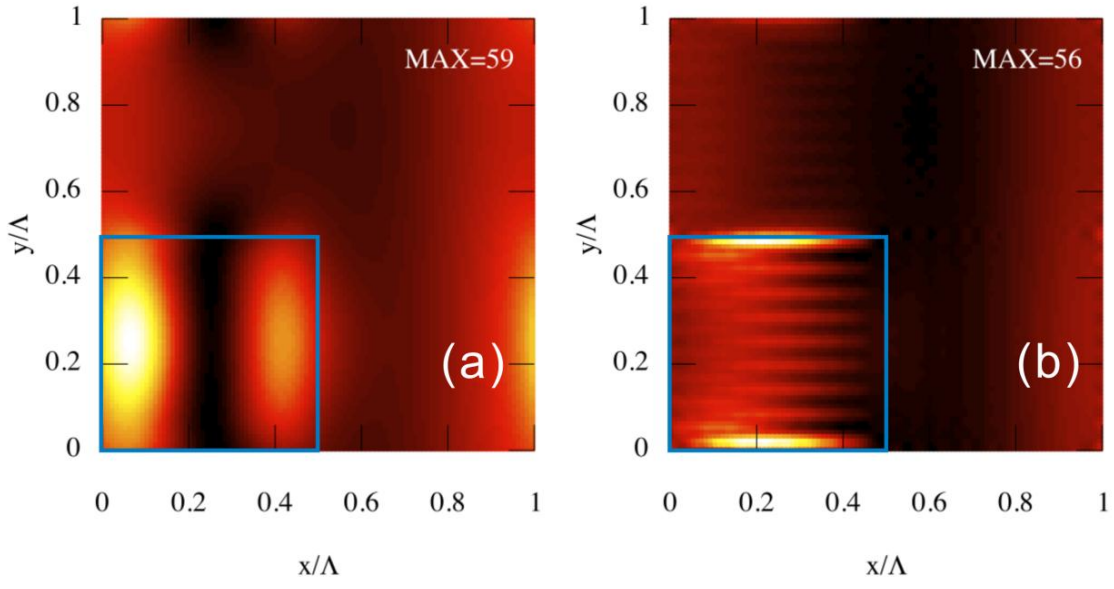

Fig 5-7, the *y*-direction magnetic field distribution for reflectance dips at 11800 cm^{-1} while $\theta = 40^{\circ}$ on the surface of silver substrate (a) and on the top surface of the nanodisk (b).

nanodisk and also the universal enhanced field on the surface. On the top surface of the nanodisk, the field distribution shows the characteristics of LSP that strong enhanced filed localized around the nanodisk. Therefore, the dip at 11800 cm^{-1} under $\theta = 40^{o}$ shows all the characteristics of MP2, SP and LSP, which indicates the dips results from the coupling of the MP2, SP and LSP modes.

This hybridized mode we have previously discussed results from the angle independence of SP modes. Hence in the case that SP cannot be supported (i.e. *s*-polarization), the coupling effect cannot be observed in the reflectance under the *s*-polarization oblique incidence as shown in Fig 5-8.

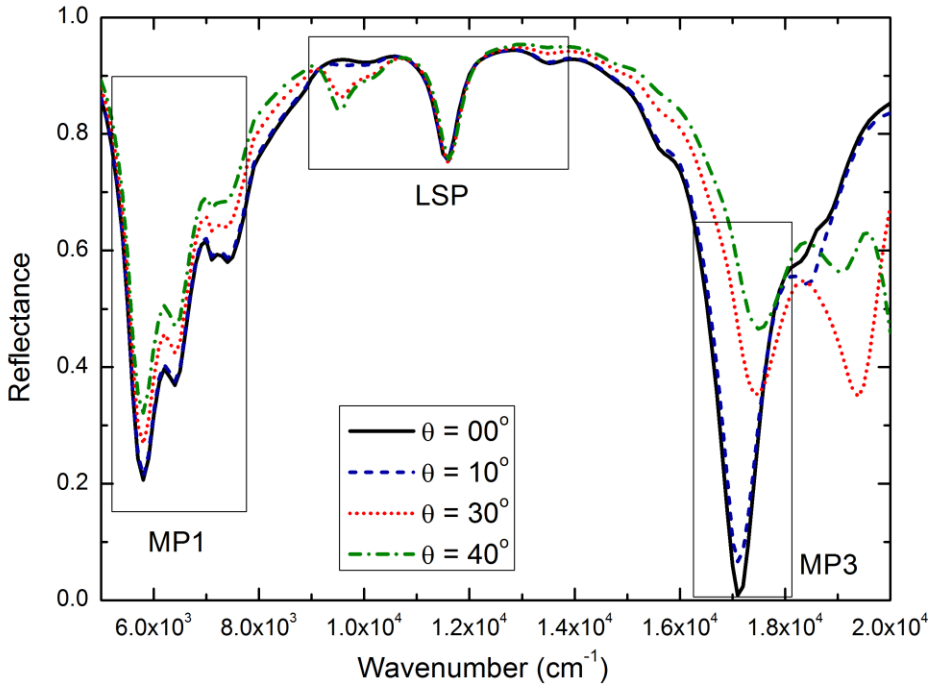

Fig 5-8, the reflectance of the proposed nanodisk-aligned multilayer structure for the different incidence angles, while the incident lights are in *s*-polarization.

5.3 ASYMMETRIC NANODISK-ALIGNED MULTILAYER

So far from our discussion, the characteristics of MP modes and LSP modes on nanodisk-aligned multilayer are similar with each other. They both depend only on the geometric shape and the intrinsic material property, while they are independent of the incidence angle and the polarization. To further distinguish LSP modes with MP modes, we introduce the asymmetric nanodisk-aligned multilayer structure, as Fig 5-9 shows. In this structure, the square nanodisk with *w* by *w* in symmetric nanodisk-aligned multilayer is replaced by the rectangular nanodisk with w_x by w_y (w_x =250 *nm*, w_y =300 *nm*).

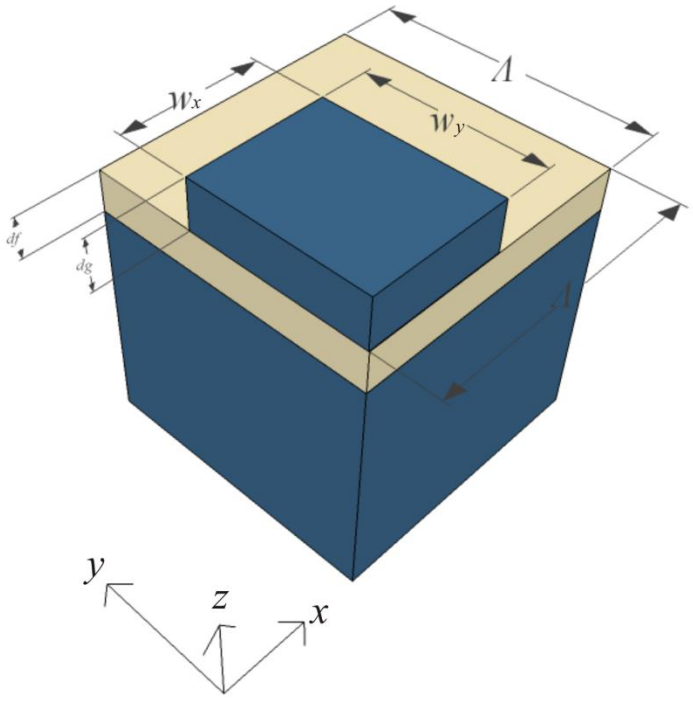

Fig 5-9. schematic of one unit cell for the asymmetric nanodisk-aligned multilayer structure. Λ *=500 nm,* d_f*=25 nm,* d_g*=30 nm,* w_x*=250 nm,* w_y*=300 nm.*

We calculate the reflectance for such structure under normal incidence both in p-polarization and s-polarization, plotted in Fig 5-10 and Fig 5-11. As we can see, for the p-polarization, MP modes, including MP1 round 6000 cm^{-1} and MP3 mode around 17000 cm^{-1} remain, yet the LSP mode at 11600 is gone. On the other hand, for the s-polarization, the LSP mode at 11600 remains unchanged, yet the MP modes, both MP1 and MP3, shift to a lower frequency.

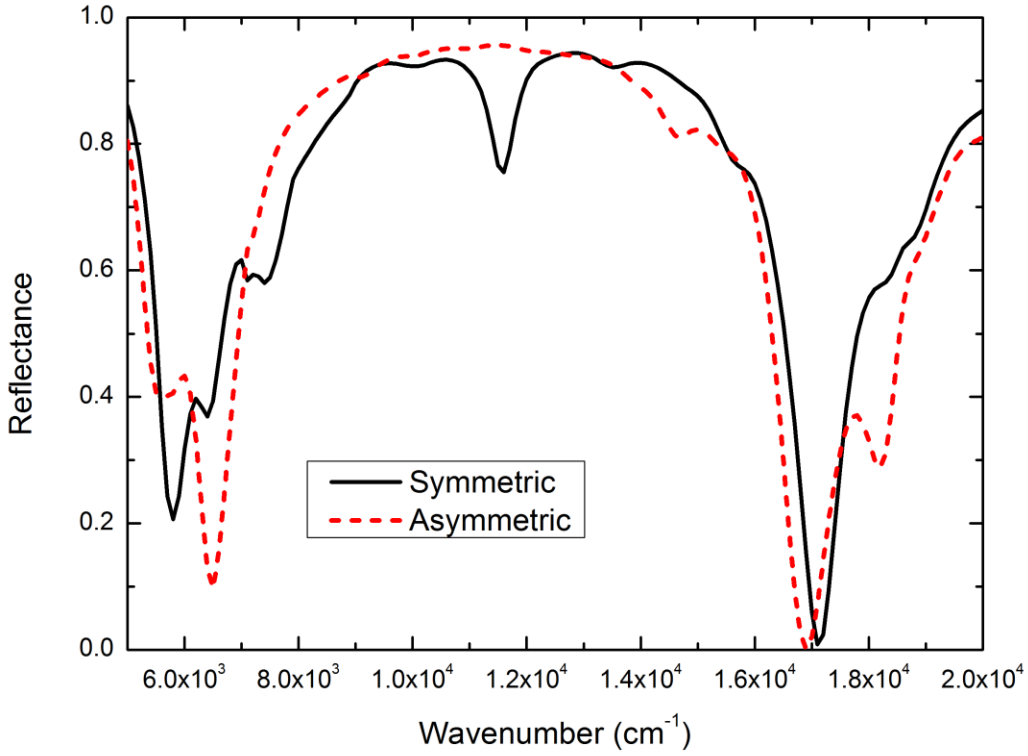

Fig 5-10, reflectance of the asymmetric nanodisk-aligned multilayer for the normal incidence (red) compared with the reflectance of symmetric nanodisk-aligned multilayer for the normal incidence (black). The incidence is in *p*-polarization.

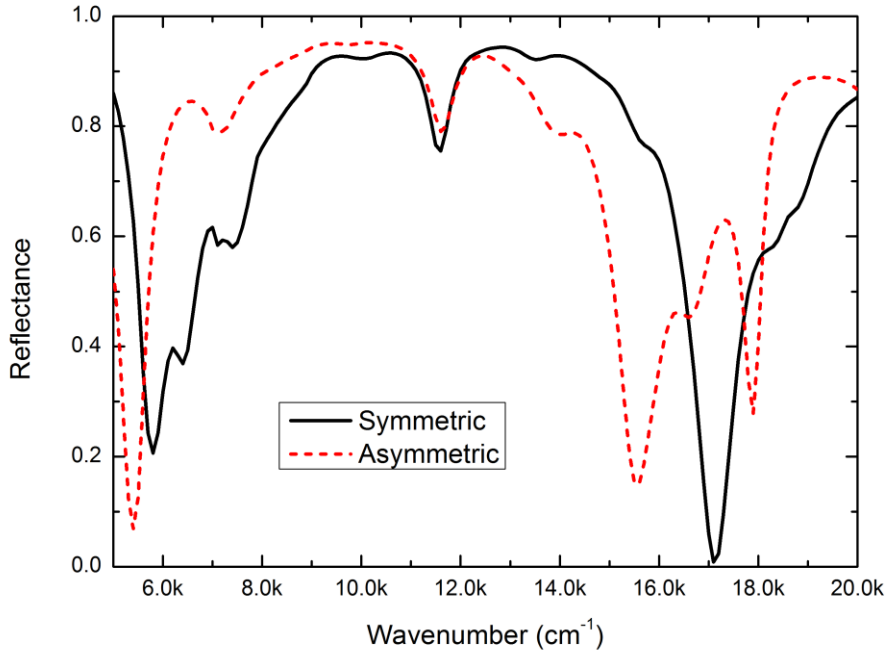

Fig 5-11, reflectance of the asymmetric nanodisk-aligned multilayer for the normal incidence (red) compared with the reflectance of symmetric nanodisk-aligned multilayer for the normal incidence (black). The incidence is in *s*-polarization.

We can understand this as follows. The direction of resonance is defined as the direction along which the anti-nodes of the resonance align. The direction of MP resonance is parallel to the direction of electric field, as we can see in the field distribution on the surface of silver substrate for MP resonance such as Fig 5-7(a). Oppositely, the direction of LSP resonance is vertical to the direction of electric field, which is shown in the field distribution of LSP such as Fig 5-7(b). Thus, the key parameter affecting MP resonance is the geometry length along the direction of the electric field, while the determinate parameter for LSP resonance is the geometry length perpendicular to the direction of electric field. Therefore, when the asymmetric nanodisk-aligned multilayer is under *p*-polarization incidence, electric field is along *x*-direction. And the

geometry length along x-direction w_x is unchanged with symmetric nanodisk-aligned multilayer w. Hence the MP resonance should also be unchanged for p-polarization. Yet for LSP resonance the geometry length perpendicular to electric field w_y varies from w, thus the LSP resonance is different for asymmetric nanodisk-aligned multilayer under p-polarization incidence. In the contrary, while symmetric nanodisk-aligned multilayer is under s-polarization, the electric field is along y-direction. So LSP is determined by w_x and MP is determined by w_y. Therefore the LSP mode stays unchanged at the same time that MP modes shift to lower frequency because w_y is larger than w for symmetric nanodisk-aligned multilayer.

By investigating the reflectance of asymmetric nanodisk-aligned multilayer, we know MP modes are affected by the geometry parameter along the electric field while LSP modes are determined by the one perpendicular to the electric field. This finding helps us understand more about the mechanism of MP and LSP resonance and offers another degree of freedom to tailor radiative property of renewable energy applications.

We demonstrate in this chapter that the proposed nanodisk-aligned multilayer structure can support not only MP modes but also SP modes and LSP modes. Moreover the SP modes can be coupled with MP modes and LSP modes by changing the incidence angle. The dominant parameters for MP and LSP modes are in the different directions which are perpendicular to each other. All those characteristics employ us more possibility to manipulate the radiative properties of nanostructures both in the near-field and far-field, which can be used to the renewable energy applications.

6.0 CONLUSION AND FUTURE WORK

This thesis proposes a novel nanodisk-aligned multilayer structure, on which all the plasmonic resonances, SP, LSP and MP, can be excited at the same time and interact with each other, supporting the coupled modes. To numerically study the structure, the RCWA method is extended to 2D and applied to the nanodisk-aligned multilayer. The strong energy constraint of SP, LSP and MP phenomenon presents characteristic dips in the reflectance. Therefore each plasmonic mode is analyzed by investigating the reflectance of the structure under different incidence angles and polarizations. The magnetic field distributions are also calculated to verify the single modes and hybridized modes and to explore the mechanisms beneath them.

It is shown that MP1 and MP3 mode can be excited on nanodisk-aligned multilayer structure under either normal or oblique incidence, and their resonance frequencies are independent of the incidence angle and polarization. MP2 mode occurs while it is under oblique p-polarization incidence, in which case the symmetry of the resonance loops is broken.

LSP can be supported by the nanodisk in the proposed structure. Similar to MP modes, LSP modes depend only on geometry parameters and the intrinsic material properties. Hence, LSP modes are shown to be independent of the incidence angle and polarization as well.

SP mode on the other hand is demonstrated to occur only under p-polarization incidence and vary with the incidence angle. And because of the angular dependence of the SP mode, it can be coupled with MP modes and LSP modes at some specific incidence angle. The coupled MP3

and SP mode is found at the normal incident for both s-polarization and p-polarization. The coupled LSP, MP2 and SP mode exists at larger incidence angle like 30^o or 40^o for the p-polarization incidence. Those coupling effects shift the resonance frequency of the original LSP, MP and SP modes and present stronger dips in the reflectance.

The asymmetric nanodisk-aligned multilayer structure is also introduced, on which MP and LSP oscillate in different directions and are distinguishable.

To summarize, in this thesis, the proposed nanodisk-aligned multilayer structure shows the feasibility to support all-incident-angle and polarization-independent radiative property enhancement both in the near-field and far-field. These features hold great potentials in renewable energy applications, such as thermal emitter, thermal collector and photovoltaic cell. The discussion about the hybridization of the plasmonic resonances as well as the asymmetric nanodisk-aligned multilayer can enhance our understanding of the mechanism of the plasmonic modes and provide us with more degrees of freedom to manipulate the radiative property of metamaterials.

In the future, the underlying physical mechanism of the splitting of MP1 mode on the nanodisk-aligned multilayer structure needs to be investigated, which can provide us with more complete physical understanding of the system and more precise control of the MP modes. Theoretically, I propose to develop a LC circuit model for the 2D nanodisk-aligned multilayer structure to predict MP1 modes. To tailor MP and LSP resonances, nanodisks of different cross section shapes may need to be introduced and studied. Moreover, nanodisk-aligned multilayer structures with the different periodicity (e.g. hexagon and diamond) need to be present to investigate more complex hybridization modes which might support stronger coupling and broader spectral range radiative property enhancement.

REFERENCES

[1] Pendry, J. B., "Negative Refraction Makes a Perfect Lens," Phys. Rev. Lett. 85, 3966, 2000

[2] Srituravanich, W., Fang, N., Sun, C., Luo, Q., and Zhang, X., "Plasmonic Nanolithography", Nano Letters, 4 (6), 1085, 2004

[3] Mühlschlegel, P., Eisler, H. J., Martin, O. J. F., Hecht, B. and Pohl, D. W., "Resonant optical antennas," Science 308, 1607, 2005

[4] Bozhevolnyi, S. I., "Waveguiding in Surface Plasmon Polariton Band Gap Structures," Phys. Rev. Lett. 86, 14, 2001

[5] Pillai, S., Catchpole, K. R., Trupke, T., and Green, M. A., "Surface plasmon enhanced silicon solar cells," Jour. of Appl. Phys., 101, 093105, 2007

[6] Greffet, J.-J., Carminati, R., Joulain, K., Mulet, J.-P., Mainguy, S., and Chen, Y., "Coherent Emission of Light by Thermal Sources," Nature, 416, 61-64, 2002.

[7] Lee, B.J., Fu, C. J., and Zhang, Z.M., "Coherent thermal emission from one-dimensional photonic crystals," Appl. Phys. Lett. 87, 071904, 2005.

[8] Zhang, Z.M., "Nano/Microscale Heat Transfer," McGraw-Hill, New York, 2007

[9] Barnes, W. L., Dereux, A. and Ebbesen, T. W., "Surface Plasmon Subwavelength Optics," Nature 424, 824-830, 2003

[10] Degiron, A., Lezec, H.J., Yamamoto, N., Ebbesen, T.W., "Optical transmission properties of a single subwavelength aperture in a real metal," Opt. Comm., 239, 61, 2004

[11] Liu, H., Liu, Y. M., Li, T., Wang, S. M., Zhu, S. N. and Zhang, X., "Coupled magnetic polaritons in metamaterials," Phys. Status Solidi B 246, No. 7, 1397, 2009

[12] Ebbesen, T. W., Lezec, H. J, Ghaemi, H. F., Thio, T. and Wolff, P. A., "Extraordinary optical transmission through sub-wavelength hole arrays," Nature, 391, 667, 1998

[13] Hooper, I. R. and Sambles, J. R. "Surface plasmon polaritons on thin-slab metal gratings," Phys. Rev. B, 67, 235404, 2003

[14] Ghaemi, H. F., Thi, T. and Grupp, D. E., "Surface plasmons enhance optical transmission through subwavelength holes," Phys. Rev. B, 58, 11, 1998

[15] Thio, T., Pellerin, K. M., Linke, R. A., Lezec, H. J. and Ebbesen, T. W., "Enhanced light transmission through a single subwavelength aperture," Opt. Lett., 26(24), 1972, 2001

[16] Zhao, C. and Zhang, J. "Binary plasmonics: launching surface plasmon polaritons to a desired pattern," Opt. Lett., 34(16), 2417, 2009

[17] Chang, S. and Gray, S. K., "Surface plasmon generation and light transmission by isolated nanoholes and arrays of nanoholes in thin metal films," Opt. Express, 13(8), 3150, 2008.

[18] Lee, J. W., Seo, M. A. , Kang, D. H. , Khim, K. S. , Jeoung, S. C. and Kim, D. S., "Terahertz Electromagnetic Wave Transmission through Random Arrays of Single Rectangular Holes and Slits in Thin Metallic Sheets "Phys. Rev. Lett. 99, 137401, 2007

[19] Seo, M. A. , Adam A. J. L. , Kang, J. H. , Lee, J. W. , Ahn, K. J. , Park, Q. H., Planken, P. C. M. and Kim, D. S., "Near field imaging of terahertz focusing onto rectangular apertures," Opt. Express, 16(23), 20484, 2008.

[20] Yamamoto, M. , Araya, K. and Garcia de Abajo, F. J. "Photon emission from silver particles induced by a high-energy electron beam," Phys. Review B, 64, 205419, 2001

[21] Haes, A. J. and Van Duyne, R. P., "A Nanoscale Optical Biosensor: Sensitivity and Selectivity of an Approach Based on the Localized Surface Plasmon Resonance Spectroscopy of Triangular Silver Nanoparticles," J. AM. CHEM. SOC., 124, 10596, 2002,

[22] Pendry, J.B., Holden, A.J., Robbins, D.J., and Stewart, W.J., "Magnetism from Conductors and Enhanced Nonlinear Phenomena," IEEE Transactions on Microwave Theory and Techniques, 47, 2075-2084, 1999.

[23] Linden, S., Enkrich, C., Wegener, M., Zhou, J. F., Koschny, T., and Soukoulis, C. M., 2004, "Magnetic Response of Metamaterials at 100 Terahertz," Science, 306, 1351, 2004.

[24] Enkrich, C., Wegener, M., Linden, S., Burger, S., Zschiedrich, L., Schmidt, F., Zhou, J.F., Koschny, T., and Soukoulis, C.M., "Magnetic Metamaterials at Telecommunication and Visible Frequencies," Physical Review Letters, 95, 203901, 2005.

[25] Zhou, J., Economon, E. N., Koschny, T. and Soukoulis, C. M., "Unifying approach to left-handed material design," Opt. Lett., 31(24), 3620, 2006

[26] Sarychev, A. K., Shvets, G., Shalaev, V. M., "Magnetic polariton resonance," Phys. Review E, 73, 036609, 2006

[27] Chettiar, U. K., Kildishev, A. V., Klar, T. A. and Shalaev, V. M., "Negative index metamaterial combining magnetic resonators with metal films," Opt. Express, 14(17), 7872, 206

[28] Cai,W., Chettiar, U. K., Yuan, H., de Silva,V. C., Kildishev, A. V., Drachev, V. P. and Shalaev, V. M., "Metamagnetics with rainbow colors," Opt. Express, 15(6), 3333, 2007

[29] Kafesaki, M., Tsiapa, I., Katsarakis, N., Koschny, Th., Soukoulis, C. M. and Economou, E. N., "Left-handed metamaterials: The fishnet structure and its variations," Phys. Review B, 75, 2345114, 2007

[30] Valentine, J., Zhang, S., Zentgraf, T., Ulin-Avila, E. , Genov, D. A. , Bartal, G., Zhang, X. , "Three-dimensional optical metamaterial with a negative refractive index", Nature 455, 367, 2008

[31] Lee, B.J., Wang, L.P., and Zhang, Z.M., "Coherent Thermal Emission by Excitation of Magnetic Polaritons between Periodic Strips and a Metallic Film," Opt. Express, 16, 11328-11336, 2008

[32] Zhu, S. and Fu, Y., "Hybridization of localized surface plasmon resonance-based Au–Ag nanoparticles," Biomed Microdevices, 11, 579, 2009

[33] Bao, Y., Peng, R., Shu, D., Wang, M., Lu, X. , Shao, J. , Lu, W. , Ming, N. "Role of Interference between Localized and Propagating Surface Waves on the Extraordinary Optical Transmission Through a Subwavelength-Aperture Array," Phys. Rev. Lett. , 101, 087401, 2008

[34] Jackson, J. D., Classical Electrodynamics, John Wiley & Sons, Inc., New York, 1999

[35] Katsarakis, N., Koschny, T., Kafesaki, M., Economou, E. N., Soukoulis, C. M., "Electric coupling to the magnetic resonance of split ring resonators," Appl. Phys. Lett. 84, 2943, 2004

[36] Liu, N., Liu, H., Zhu, S. N., Giessen, H., "Stereometamaterials" Nature Photonics 3, 157, 2009

[37] Liu, N., Guo, H., Fu, L., Kaiser, S., Schweizer, H. and Giessen, H., "Plasmon Hybridization in Stacked Cut-Wire Metamaterials," Advanced Materials, 19, 2628, 2007

[38] Wang, F. M., Liu, H., Li, T., Zhu, S. N., and Zhang, X. "Omnidirectional negative refraction with wide bandwidth introduced by magnetic coupling in a tri-rod structure," Phys. Rev. B 76, 075110, 2007

[39] Liu, H., Liu, Y. M., Li T., Wang, S. M., Zhu, S. N. and Zhang, X., "Coupled magnetic polaritons in metamaterials," Phys. Status Solidi B 246, 1397, 2009

[40] Moharam M. G., Gaylord, T. K., "Rigorous coupled-wave analysis of planar-grating diffraction" J. Opt. Soc. Am. 71, 811, 1981

[41] Moharam M. G., Gaylord, T. K., "Rigorous coupled-wave analysis of metallic surface-relief gratings," J. Opt. Soc. Am. A 3, 1780, 1986

[42] Chen, Y. –B., Tan, K.-H., "The profile optimatioan of periodic nan-structure for wavelength-selective thermophotovoltaic emitters," Int. J. Heat and Mass Transfer 53, 5542, 2010

[43] Raether, H., "Surface Plasmons on Smooth and Rough Surfaces and on Gratings," Springer-Verlag, 1988